Conf-950201--13

PNL-SA-26013

INTERFACIAL SEGREGATION AND DEFORMATION OF SUPERPLASTICALLY DEFORMED Al-Mg-Mn ALLOYS

J. S. Vetrano
C. A. Lavender
S. M. Bruemmer

March 1995

Presented at the
The Minerals, Material, and Metals Society Annual Conference
February 12-16, 1995
Las Vegas, Nevada

Prepared for
the U.S. Department of Energy
under Contract DE-AC06-76RLO 1830

Pacific Northwest Laboratory
Richland, Washington 99352

DISCLAIMER

Portions of this document may be illegible in electronic image products. Images are produced from the best available original document.

Interfacial Segregation and Deformation of Superplastically Deformed Al-Mg-Mn Alloys

John S. Vetrano, Curt A. Lavender and Stephen M. Bruemmer
Pacific Northwest Laboratory, Richland, WA 99352

Abstract

Microstructural and microchemical studies have been carried out on superplastically deformed Al-Mg-Mn (AA5083-type) alloys. Grain boundary composition was measured using a Scanning Auger Microprobe (SAM) and an Analytical Transmission Electron Microscope (ATEM), while conventional TEM was used for microstructural evaluation. Non-equilibrium segregation of Si to grain boundaries following deformation was measured by both techniques. Significant interfacial Si enrichment was only detected in gage sections of tensile specimens after uniaxial strains from 50 to 200%. Grip regions which experience identical thermal histories, but without plastic deformation, did not reveal Si segregation. Selected samples also showed a slight depletion of Mg at grain boundaries after deformation. The only reproducible observation of equilibrium segregation was in Zr-modified alloys, where Sn was detected by SAM in both the deformed and undeformed sections of the sample. Microstructural analysis documented subgrain formation and subgrain-precipitate interactions during superplastic deformation. In addition, many grain boundaries and precipitate interfaces contained small (5 to 20 nm) voids. Compositional analysis of these nano-voids revealed that they were enriched in Mg with the adjacent boundary regions correspondingly depleted.

Introduction

The process of grain boundary sliding (GBS) is the dominant mode of deformation during fine-grain superplasticity (1), whereas cavitation is the dominant mode of failure (2). Investigation of these two effects has centered primarily on "micron-scale" GBS and cavity formation measurements, typically performed in either the scanning electron microscope or by optical metallography. Nano-scale measurements of grain boundary structure and composition have generally not been attempted. Only recently has the local composition at grain boundaries in superplastic metals been investigated and analyzed in terms of GBS and cavitation (3-6). Vetrano *et al.* (3) examined the change in grain boundary composition in Al alloy 5083 following GBS and identified impurity segregation. Nieh *et al.* (4) and Koike *et al.* (5) considered that segregation of impurities may form a liquid phase to assist in the accommodation of strain in high strain-rate superplasticity of composites. In addition, Park *et al.* (6) found a deleterious effect of impurities on the deformation and cavitation of a Zn-22%Al alloy, though they have not measured the impurity concentration at the boundaries. Research on materials undergoing creep deformation have shown that solute segregation can affect GBS, grain growth and cavitation through processes such as solute-point defect interactions and surface free energy changes (7).

A superplastic alloy that lends itself to the study of grain boundary segregation and deformation is Al-4.5Mg-0.8Mn (AA5083), which is a non-heat-treatable alloy widely available in a commercial grade, and also produced in a superplastic grade. The mechanical behavior of this alloy and its derivatives have been the subject of several recent papers (8-13), and preliminary assessment of grain boundary chemistry found evidence of deformation-induced segregation (3).

Though research on deformation-induced segregation is limited, there have been several studies carried out on the segregation of Mg in Al-Mg alloys under purely thermal conditions (14-17). Lea and Molinari (14) treated the segregation of Mg in Al-Mg alloys both theoretically and experimentally, via Auger Electron Spectroscopy (AES), and noted that Mg will quickly segregate to a free surface, then evaporate if the sample is in a vacuum, or oxidize if the oxygen concentration is sufficient. Studies of Al-Mg (15) and Al-Zn-Mg (16,17) alloys in the "as-quenched" condition have observed an enrichment in Mg at the grain boundaries.

In this paper we will present results on the equilibrium and non-equilibrium segregation of impurities and major alloying elements during superplastic deformation of 5083-based alloys. Compositional analysis was carried out by both AES and Energy Dispersive Spectroscopy (EDS). Complementary microstructural assessments were made in the transmission electron microscope (TEM). More detail on the precipitate structure and superplastic deformation behavior of these alloys is presented elsewhere (8,9).

Experimental

Three 5083-base alloys will be evaluated: Al-4.5Mg-0.8Mn, Al-4.5Mg-0.8Mn-0.2Zr, and Al-4.5Mg-1.6Mn-0.2Zr. The same commercial "high" purity base chemistry was used for all alloys with relatively low Fe (0.08 wt%) and Si (0.03 wt%) impurity levels. These heats were supplied by the Kaiser Center for Technology (KCT) as

75-mm-thick DC cast ingots. The relatively slow cool during the casting process results in typically non-coherent Al-Zr precipitates that are not influenced by the subsequent warm/cold working of the ingot. (8,9)

Dog-bone-shaped tensile specimens with thicknesses of either 1.8 mm (for AES) or 0.6 mm (for TEM) were mechanically tested in an MTS servo-hydraulic tensile testing machine at temperatures from 450-550°C, strains from 0-200%, and strain rates from $4x10^{-4}$ s^{-1} to $1x10^{-2}$ s^{-1}. When the desired strain was reached the samples were quenched under load by spraying a Freon-type liquid (chlorodifluoromethane) directly on the surface. A cooling rate of approximately 75°C s^{-1} was measured for the thicker specimens by attaching a thermocouple to the back side of a sample. The thinner samples should have a slightly faster quench rate.

Specimens suitable for fracture in a PHI 660, high-resolution Scanning Auger Microprobe (SAM) were prepared from both the gage and grip sections of the tested materials and fractured in situ via Ga-induced intergranular embrittlement (3). Examination in the SAM was limited to about three hours by the gradual oxidation of the sample surface, allowing analysis of 15-20 boundary facets. Compositional measurement in the SAM is sensitive to the top two or three atomic layers, and the quantitation is performed by measuring the peak heights of a differentiated intensity versus energy spectrum, and applying appropriate scaling factors.

Specimens for TEM analysis were prepared by punching out 3-mm disks from the as-tested samples and lightly grinding them to a thickness of approximately 200 μm. Notches were filed on the disk edge to denote the tensile direction. They were then electropolished in a Struers Tenupol twin-jet polisher with a solution of 20% $HClO_4$ in methanol at -30°C. Examination was carried out in either a JEOL 1200 or a JEOL 2010F TEM. The latter is equipped with a field-emission gun that allows quick EDS compositional analysis with a 1-nm probe size. The necessity of finding a boundary suitable for EDS (on-edge, in thin region of sample and with precipitate-free regions) limited analysis to typically 3-5 boundaries per sample.

Results

The deformation behavior of the three alloys, 5083, 5083+Zr and 5083+(Mn, Zr) have been presented elsewhere (8), but are reviewed briefly here. The alloy with additions of both Mn and Zr was superior in total elongation, strain-rate sensitivity and cavitation resistance at strain rates above $4x10^{-4}s^{-1}$, as well as having the smallest grain size. The addition of only Zr to the base 5083 alloy resulted in a slightly lower elongation at all strain rates and larger grain size. Despite the larger grains, the strain rate sensitivity of the Zr-modified 5083 was higher than the base alloy at $1x10^{-3}s^{-1}$ and at all strain levels to 200%, and exhibited less cavitation.

Analysis of the 5083 and Zr-containing alloys by SAM revealed two primary segregants. Silicon was segregated to grain boundaries in all three alloys after straining, but none was present in the grip (non-strained) sections. Though quantitative analysis is made difficult by the presence of Ga on the surface, typical concentrations were less than 7 at%. In addition, Sn was detected in the Zr-modified alloys at levels of approximately 1 at.% in both the strained and un-

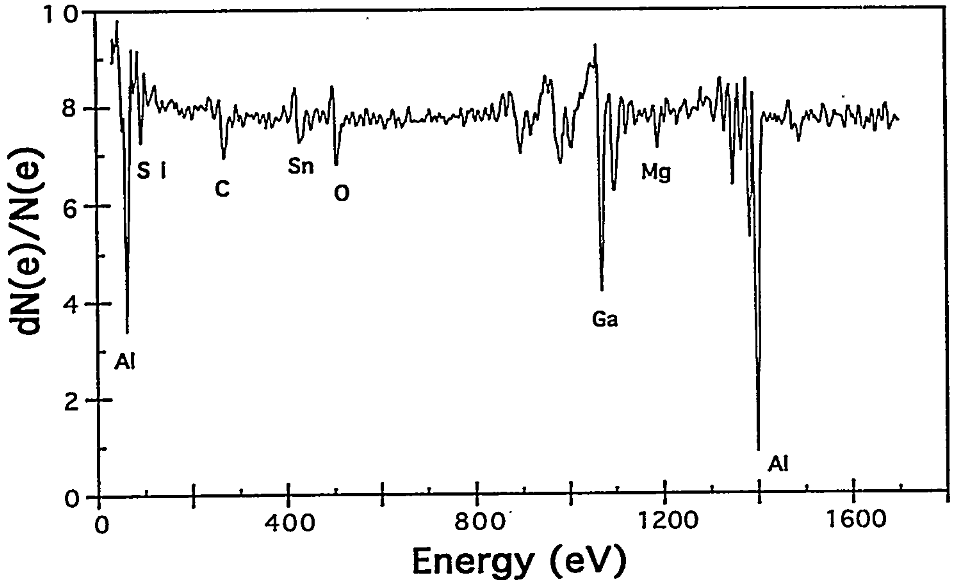

Figure 1. SAM spectrum of a superplastically deformed Zr-modified 5083 alloy revealing the presence of Si and Sn on the grain boundary.

strained portions of the sample. This indicates that it is an equilibrium segregant. A representative SAM spectrum of a grain boundary analysis in a Zr-modified 5083 alloy following deformation at 550°C to a strain of 200% is shown in Figure 1. The amount of both Si and Sn showed extensive grain-to-grain variability and they were not present on every grain boundary facet. Zirconium was occasionally seen on grain boundaries in the Zr-modified alloys; most likely due to the presence of an Al_3Zr precipitate on the boundary.

Grain boundary compositional analysis via TEM-EDS confirmed the deformation-induced segregation of Si, though at a lower level than detected in the SAM. In addition, a slight depletion of Mg was identified at most boundaries in deformed samples. An example of a composition profile measured across a grain boundary is presented in Figure 2. Distinct concentration differences were consistently detected at the grain boundary in relation to adjacent matrix regions.

Microstructural analysis of 5083 and 5083+(Mn,Zr) (deformed to 100% at a strain rate of $1x10^{-3}s^{-1}$ and a temperature of 450°C) was carried out in the TEM. In general, there was little difference in the deformation structure between the two alloys. Dislocation activity was observed in the grain centers and along grain boundaries, indicating that much of the dislocation activity was quenched in. Most grains showed some type of dislocation organization in the form of either partially or completely developed subgrains. As can be seen in Figure 3, there was a strong attraction between subgrains and the submicron-sized Al_6Mn particles. Because the particles were generally decorated with dislocations, it is speculated that they play a role in the development of the subgrain structure through the capture of moving dislocations. Little influence of the Al_3Zr particles was noted; however, this is not unexpected as they are distributed inhomogeneously throughout the microstructure and are incoherent.

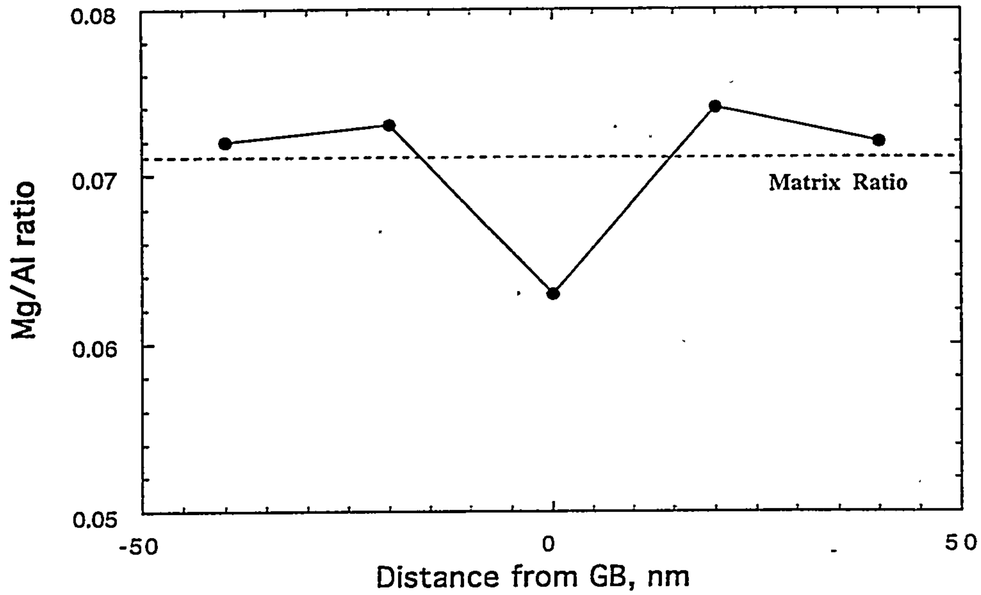

Figure 2. Composition gradient measured across a grain boundary in deformed 5083 by TEM-EDS using an incident probe size of 1 nm.

Figure 3. TEM micrograph demonstrating the particle-subgrain interactions in a superplastically deformed 5083 alloy. The particle is Al_6Mn. Tensile direction is indicated.

An interesting feature of these samples that was revealed in the TEM was the presence of "nano-voids" on grain boundaries and precipitate interfaces. These voids, which were between 5-20 nm in diameter and were observed on approximately 25% of the grain boundaries, can be seen in Figure 4. Extensive TEM analysis of these features including over- and under-focus imaging, tilting and nano-beam diffraction have confirmed that they are voids and not small precipitates. Figure 4a shows a grain boundary in a non-diffracting, over-focus condition that reveals the void nature of the features, whereas in Figure 4b the same boundary is tilted slightly to a strongly diffracting condition revealing that

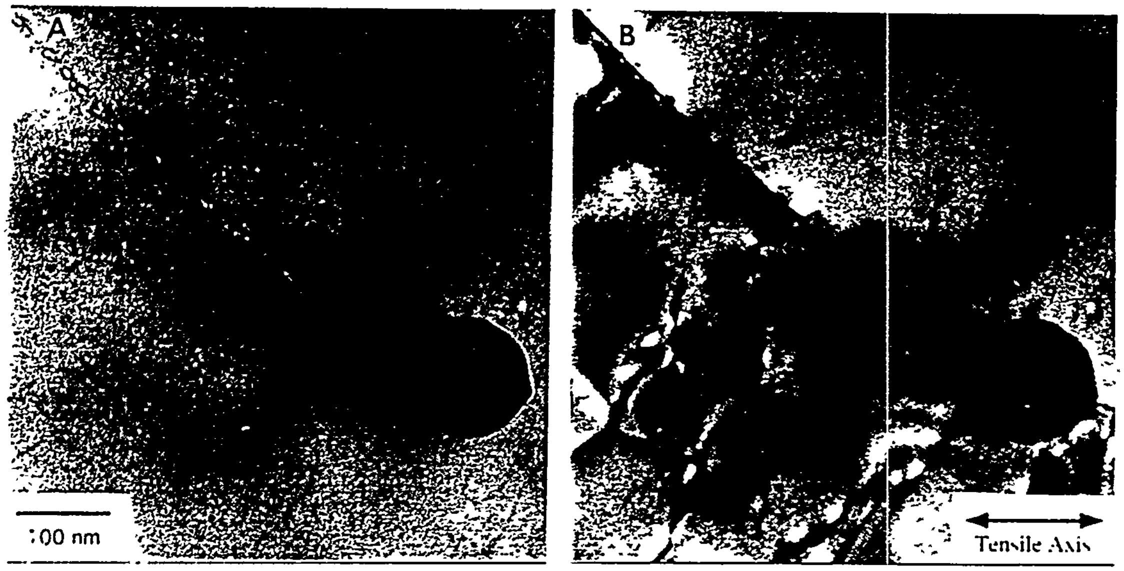

Figure 4. a) Grain boundary in Zr-modified 5083 following superplastic deformation showing nano-voids. b) Same boundary, now with one grain strongly diffracting to reveal the stress fields associated with the nano-voids.

these features are also strain centers. Many of the nano-voids were associated with lattice dislocations intersecting the grain boundary. Compositional analysis of the nano-voids with EDS indicates that they are enriched in Mg over the adjacent grain boundary by ~40% (to >6 wt%). These features were not present on the grain boundaries of deformed, air-cooled samples and it is not clear at this time whether they were present at the deformation temperature or were formed during the quench.

Discussion

The complementary nature of SAM and TEM-EDS analysis can be seen in the above analysis of the microstructure and microchemistry of grain boundaries in superplastically deformed 5083-based alloys. SAM has a high resolution for elements enriched within a few atom distances of the surface and is the most sensitive technique to detect segregants localized within the grain boundary plane if intergranular fracture can be produced in-situ. Many exposed boundaries can be analyzed in the same sample to determine grain-to-grain variability, but with little microstructural characterization of individual boundaries. In contrast, the fine-probe analysis possible in the TEM lends itself to a detailed comparison of local microchemistry and microstructural features, as well as the direct measurement of composition profiles across regions of interest.

Grain boundaries act as both sources and sinks of point defects, and they also represent low-energy sites for solute atoms that are not stable in the bulk. The processes of GBS and accommodation during superplastic deformation likely serve to drive certain solute atoms toward (or away from) the grain boundaries. A recent theory of superplasticity (18) which considers the grain boundary to be in a special highly-excited state due to the accommodation of lattice dislocations points to a grain boundary structure that would allow further attraction and accommodation of impurities. Hondros and Seah (7) pointed out that even impurities present at the ppm level can enrich to significant concentrations at grain boundaries due to equilibrium segregation processes.

Microstructural examination of 5083 and 5083+(Mn,Zr) revealed no significant variation in their dislocation or grain boundary structure, which points to a compositional effect as perhaps being a more dominant contribution to their differences in superplastic response. The presence of Si and Sn at the grain boundaries has the potential to affect the mechanical properties, as does the reduction in Mg. In particular, Sn may form a liquid phase or strongly enhance interfacial diffusion at the deformation temperature. A grain boundary liquid phase may be beneficial, by relieving stresses (19), or deleterious by causing grain decohesion, depending on the amount present. In addition, though the exact mechanisms of GBS are not known, the depletion of Mg at the boundaries has the potential to reduce solute drag on grain boundary dislocations and thereby serve to ease sliding. The presence of equal amounts of Sn at boundaries in the grip and gage sections of the samples indicates that it is an equilibrium segregant. The enrichment of Si and the reduction in Mg content of the boundaries only after straining, however, indicates that this segregation is being driven by the deformation process.

Another area where segregation may play a role is the formation and stabilization of a free surface such as in voids. Data from Lea and Molinari (14) indicate that Mg should saturate a free surface in seconds at these temperatures, leading to the formation of a Mg-rich region around the voids. This could act to strengthen the region and retard further void growth, though it would also inhibit further sliding along that grain boundary.

Conclusions

Segregation of impurities and major alloying elements is observed following superplastic deformation. Silicon was present in all alloys tested after deformation. SAM analysis of the Zr-modified 5083 detected Sn both with and without deformation. In addition, TEM-EDS analysis revealed a depletion of Mg at the grain boundaries. Microstructural analysis indicated that the submicron Al_6Mn precipitates dominate the boundary and dislocation pinning, with the Al_3Zr particles having only a minor effect. Nano-voids were observed on approximately 25% of the grain boundaries following deformation, and EDS analysis indicated that they were enriched in Mg. The presence of Sn is a possible aid in the superplastic deformation of the Zr-modified alloys.

Acknowledgments

The assistance of Dave Criswell with the mechanical testing is acknowledged. This work was supported by the Materials Sciences Division, Office of Basic Energy Sciences, U.S. Department of Energy (DOE) under Contract DE-AC06-76RLO 1830.

References

1. T.G. Langdon, "The Role of Grain Boundaries in High Temperature Deformation," Mat. Sci. and Eng., **A174** (1994) p. 225.

2. A.H. Chokshi, "Cavitation Behavior during Superplastic Deformation," in Superplasticity in Advanced Materials, ed. by S. Hori, M. Tokizane and N. Furushiro (JSRS, Osaka, Japan 1991), p. 171.

3. J.S. Vetrano, C.A. Lavender and S.M. Bruemmer, "Impurity Segregation During Superplastic Deformation of Al-Mg-Mn Alloys," in Proceedings of ICSAM '94, Mat. Sci. Forum (Trans Tech Publ., Switzerland).

4. T.G. Nieh, J. Wadsworth and T. Imai, "A Rheological View of High Strain Rate Superplasticity in Alloys and Metal Matrix Composites," Scripta Metall. mater. **26** (1992) p. 703.

5. J. Koike, M.Mabuchi and K.Higashi, "Partial Melting and Segregation Behavior in a Superplastic Si_3N_4/Al-Mg Alloy Composite;" J. Mater. Research, **10** (1995) p. 133.

6. K.-T. Park *et al.*, "The Effect of Impurities on Ductility and Cavitation in the Superplastic Zn-22% Al Alloy," Mat. Sci. and Eng. **A188** (1994) p. 59.

7. E.D. Hondros and M.P. Seah, "Segregation to Interfaces" Int. Metals Rev., , Dec. (1977) p. 262.

8. C.A. Lavender *et al.*, "Development of Superplasticity in 5083 Aluminum with Additions of Mn and Zr," in Proceedings of ICSAM '94, Mat. Sci. Forum (Trans Tech Publ., Switzerland).

9. J.S. Vetrano, C.A. Lavender, M.T. Smith and S.M. Bruemmer, "Effect of Precipitate Structure on Hot Deformation of Al-Mg-Mn Alloys," in Advances in Hot Deformation Textures and Microstructures, edited by J.J. Jonas, T.R. Bieler and K.J. Bowman (TMS, Pennsylvania 1994), p. 223.

10. F.Li, W.T. Roberts and P.S. Bate, "Dislocation Distributions in an Al-4.5%Mg Alloy During Superplastic Deformation," Scripta Met. et Mat. **29** (1993) p. 875.

11. F.Li, "On the Origin of the High Strain Rate Sensitivity in a Superplastic Al-4.5%Mg Alloy," Scripta Met. et Mat., **32** (1995) p. 463.

12. H. Iwasaki *et al.*, "Superplastic Deformation Characteristics of 5083 Aluminum Alloy," Superplasticity in Adv. Mat., ed. by S. Hori, M. Tokizane and N. Furushiro, p.447 (1991).

13. H. Imamura and N. Ridley, "Superplastic and Recrystallisation Behaviour of a Commercial Al-Mg Alloy 5083," *ibid*, p. 453.

14. C. Lea and C. Molinari, "Magnesium Diffusion, Surface Segregation and Oxidation in Al-Mg Alloys," J. Mat. Sci., **19** (1984) p. 2336.

15. T. Malis and M.C. Chaturvedi, "Grain Boundary Segregation in an Al-8-wt% Mg Alloy," J. Mat. Sci., **17** (1982) p. 1479.

16. P. Doig, J.W. Edington and M.H. Jacobs, "MIcroanalysis Across Grain Boundaries in Aluminum Alloys," Philos. Mag **31** (1975) p. 285.

17. J.M. Chen *et al*, "Grain Boundary Segregation of an Al-Zn-Mg Ternary Alloy," Met. Trans., 8A (1977) p. 1935.

18. V.N. Perevezentsev, V.V. Rybin and V.N. Chuvil'deev, "The Theory of Structural Superplasticity I-III," Acta metall. mater., **40** (1992) p. 887.

19. M. Mabuchi, K. Higashi and T.G. Langdon, "An Investigation of the Role of a Liquid Phase in Al-Cu-Mg Metal Matrix Composites Exhibiting High Strain Rate Superplasticity," Acta metall. mater., **42** (1994) p. 1739.